ARL-TR-9087 ● SEP 2020

DEVCOM ARMY RESEARCH LABORATORY

Back-to-Back Diplexers for Nonlinear Junction Detection

by Gregory Mazzaro, Kyle Gallagher, Arthur Harrison, Getachew Kirose, and Kelly Sherbondy

NOTICES

Disclaimers

The findings in this report are not to be construed as an official Department of the Army position unless so designated by other authorized documents.

Citation of manufacturer's or trade names does not constitute an official endorsement or approval of the use thereof.

Destroy this report when it is no longer needed. Do not return it to the originator.

ARL-TR-9087 ● SEP 2020

Back-to-Back Diplexers for Nonlinear Junction Detection

Kyle Gallagher, Arthur Harrison, Getachew Kirose, and Kelly Sherbondy
Sensors and Electron Devices Directorate, CCDC Army Research Laboratory

Gregory Mazzaro
The Citadel, The Military College of South Carolina

REPORT DOCUMENTATION PAGE

Form Approved
OMB No. 0704-0188

1. REPORT DATE *(DD-MM-YYYY)*	2. REPORT TYPE	3. DATES COVERED (From - To)
September 2020	Technical Report	1 March 2020–31 August 2020

4. TITLE AND SUBTITLE
Back-to-Back Diplexers for Nonlinear Junction Detection

5a. CONTRACT NUMBER

5b. GRANT NUMBER

5c. PROGRAM ELEMENT NUMBER

6. AUTHOR(S)
Gregory Mazzaro, Kyle Gallagher, Arthur Harrison, Getachew Kirose, and Kelly Sherbondy

5d. PROJECT NUMBER

5e. TASK NUMBER

5f. WORK UNIT NUMBER

7. PERFORMING ORGANIZATION NAME(S) AND ADDRESS(ES)
CCDC Army Research Laboratory
ATTN: FCDD-RLS-RM
Adelphi, MD 20783-1138

8. PERFORMING ORGANIZATION REPORT NUMBER
ARL-TR-9087

9. SPONSORING/MONITORING AGENCY NAME(S) AND ADDRESS(ES)

10. SPONSOR/MONITOR'S ACRONYM(S)

11. SPONSOR/MONITOR'S REPORT NUMBER(S)

12. DISTRIBUTION/AVAILABILITY STATEMENT
Approved for public release; distribution is unlimited.

13. SUPPLEMENTARY NOTES
ORCID ID(s): Gregory Mazzaro, 0000-0001-5814-7425 ; Kyle Gallagher, 0000-0002-9450-1767 ; Kelly Sherbondy, 0000-0003-4730-3706

14. ABSTRACT
To determine if a radar target possesses a nonlinear (harmonic) response, it is necessary to perform a wideband sweep of transmit frequencies while capturing a harmonic of those frequencies. The transmission must be high power and must contain minimal system-generated harmonics; the reception is at low power and must contain minimal residual transmit-probe energy. A novel arrangement of diplexers accomplishes these objectives. Two 4U metallic enclosures, containing enough diplexer pairs to sweep the transmit frequencies across the ultra-high-frequency and long-wave (L) bands, have been fabricated. This report contains figures that demonstrate how to configure the diplexers for transmit and/or receive, and data that quantify the performance of these diplexers for five separate but adjacent frequency bands.

15. SUBJECT TERMS
nonlinear, junction, harmonic, detection, radar, diplexer

16. SECURITY CLASSIFICATION OF:			17. LIMITATION OF ABSTRACT	18. NUMBER OF PAGES	19a. NAME OF RESPONSIBLE PERSON
a. REPORT	b. ABSTRACT	c. THIS PAGE			Gregory Mazzaro
Unclassified	Unclassified	Unclassified	UU	23	19b. TELEPHONE NUMBER (Include area code) (301) 394-5759

Contents

List of Figures

List of Tables

1. Introduction to Nonlinear Junction Detection

Nonlinear junction detection (NLJD) is currently being applied for security and defense, for example, to perform countersurveillance.[1–4] In this arena, relevant targets are difficult to detect because, under illumination by a traditional radar wave, the amount of electromagnetic (EM) energy reflected from them is much smaller than that reflected from nearby clutter. Thus, traditional radars generally cannot "see" nonlinear junctions, especially those that are buried or otherwise intentionally obscured. However, such junctions have the unique property of generating EM energy at frequencies different from those that illuminate them. Reception of frequencies different from the original transmit set indicates the presence of a nonlinear target.

The NLJD concept is illustrated in Fig. 1. The transmit (Tx) antenna broadcasts an EM wave into an environment that may contain a junction. The Tx probe contains a set of frequencies $\{f_{Tx}\}$. Components containing nonlinear junctions (such as the diode illustrated) capture some of this wave and distort it, generating frequencies that are not part of the original transmitted set. A power-series model[5–7] is often used to mathematically describe the conversion of the transmitted probe frequencies to the new frequencies that may be captured by the receive (Rx) antenna $\{f_{Rx}\}$. For harmonic NLJD, typically a single frequency is transmitted: f_0.[8–13] Consequently, harmonics of that frequency are received: $2f_0$, $3f_0$, and so on.

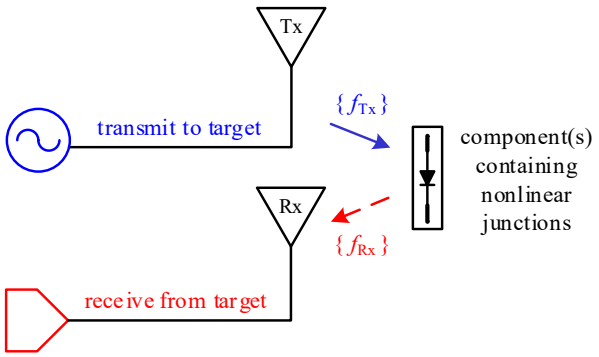

Fig. 1 Illustration of the NLJD concept: the Tx antenna emits a wave toward the nonlinear component(s). A new wave reflects from the component(s) carrying new frequencies that are not part of the Tx set. The Rx antenna captures the wave that arrives back at the detector.

A link-budget equation relating power transmitted at f_0 to power received at $2f_0$ has been derived for NLJD (i.e., "nonlinear radar").[14,15] Experimental results indicate that a much higher Tx power is required for a nonlinear sensor to establish a signal-to-noise ratio (SNR) comparable to that of traditional linear radar, assuming the same standoff distance.[16,17] Although the energy received by the nonlinear sensor

is miniscule, the frequencies produced by nonlinear junctions are vastly different from the original Tx set. In contrast, most materials found in nature are linear, so they do not exhibit this change of frequency. Thus, the key advantage of using NLJD to sense nonlinear junctions (compared to using traditional radar) is high clutter rejection.

For consistency with standard radar terminology, hereafter in this report, a nonlinear junction (or a device containing a collection of nonlinear junctions) is referred to as a "target".

2. Clutter Rejection Achieved by Passive Filtering

To achieve an adequate SNR for NLJD, it is necessary to transmit high power to the target. Unfortunately, generating high peak power necessarily generates distortion in the Tx waveform.[18] For harmonic NLJD, this distortion manifests as harmonics that (if they were absent from the Tx waveform) would map to the target reflection only. The harmonic distortion generated by the transmitter, if not adequately filtered or cancelled[19,20] before transmission, either 1) is emitted from the Tx antenna and reflects from linear clutter in the environment, which generates false alarms, or 2) couples directly from the transmitter to the receiver, which masks reflections from weaker (usually distant) targets.

Therefore, for NLJD, the Tx signal must be strongly filtered before it leaves the Tx antenna. Researchers usually include a lowpass filter (LPF) as part of their transmitter architecture.[21,22] For continuous-wave (CW) transmissions where the operational bandwidth of the signal may be made arbitrarily narrow, bandpass filtering may be implemented instead.[11,23] Those references that explicitly discuss filter specifications report rejection of self-generated harmonics ($2f_0$ and above) by 50 dB or more.[10,24] Thus, the aforementioned high degree of clutter rejection possible for harmonic NLJD is achieved (in part) by passive filtering, as illustrated in Fig. 2.

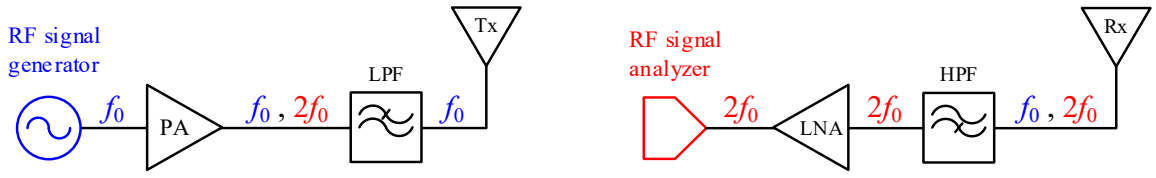

Fig. 2 Passive filtering implemented in the transmitter after the power amplifier (PA) (lowpass) and in the receiver before the low-noise amplifier (LNA) (highpass)

The probe signal for the target originates at the RF signal generator. For laboratory experiments, this is often an instrument such as the Keysight N9310A. The target

response is captured by the RF signal analyzer, which may be an instrument such as the Keysight N9320B.

In the transmitter, the high power for the Tx probe-frequency f_0 is produced by the PA. This amplification generates harmonics (e.g., $2f_0$). These harmonics are removed/reflected by the LPF so that only the undistorted probe-frequency f_0 arrives at the Tx antenna and is emitted toward the target.

Even at a relatively short standoff distance of 3 m, a typical response received at $2f_0$, for a transmit power of 1 W, is less than –80 dBm.[16] For this reason, a harmonic receiver requires a high degree of amplification and a high sensitivity. Often, the amplification is split across multiple LNAs.[25] References that discuss LNA specifications report a minimum total amplification of 45 dB in the Rx chain.[1]

Because the amplification is very high and the detector is very sensitive, filtering before each LNA is necessary to prevent the Tx signal from coupling further into the receiver and causing saturation of the detector. For a signal with an appreciable bandwidth (pulsed, stepped, chirped), the Tx probe is removed/reflected by a highpass filter (HPF).[24] For CW transmission and reception, bandpass filtering is permissible.[10,11,26] Filter specifications for harmonic receivers have been reported with rejections at f_0 equal to or greater than 76 dB.[1,25]

The goals of the present work were to 1) design a bank of coupled lowpass and highpass filters to easily switch between different frequency bands while testing the harmonic NLJD responses of different targets, and 2) implement enough filters to probe each target with a continuous band of Tx frequencies: f_0 = 300 MHz to 2 GHz (i.e., to receive harmonic responses from $2f_0$ = 600 MHz to 4 GHz).

3. Harmonically Related Diplexers

To simultaneously achieve adequate lowpass behavior in the transmitter and adequate highpass behavior in the receiver, three rules of thumb are followed[27,28] and illustrated in Fig. 3:

- The Tx (low) and Rx (high) passbands must not overlap: $f_{end} < M \cdot f_{start}$.
- The LPF should be selected with minimal loss in the passband $f_{start} < f_0 < f_{end}$ and no less than 50 dB of insertion loss in the stopband $M \cdot f_{start} < M \cdot f_0 < M \cdot f_{end}$.
- The highpass filter should be selected with minimal loss in the passband $M \cdot f_{start} < M \cdot f_0 < M \cdot f_{end}$ and no less than 70 dB of insertion loss in the stopband $f_{start} < f_0 < f_{end}$.

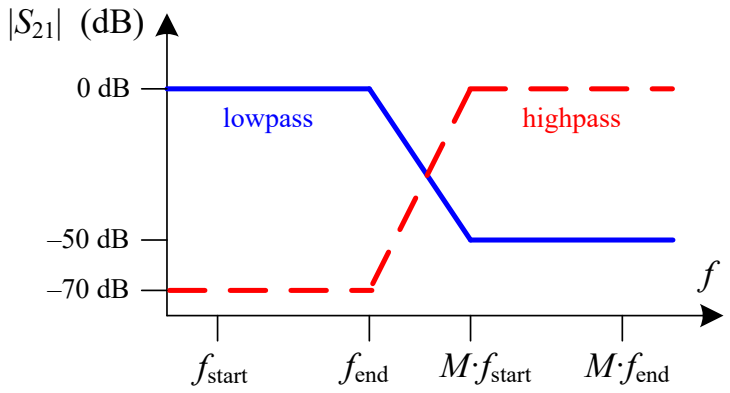

Fig. 3 Desired *S*-parameters (transmission coefficient S_{21}) for fixed filters in a harmonic NLJD: the Tx band starts at f_{start} and ends at f_{end}, while the Rx band starts at $M \cdot f_{start}$ and ends at $M \cdot f_{end}$. The low and high passbands do not overlap.

To cover the full Tx band f_0 = 300 MHz to 2 GHz while minimizing the number of discrete lowpass/highpass pairs that must be fabricated, several frequency sub-bands were chosen. These five bands are listed in Table 1. The desired (ideal) frequency bands are listed in the second and fourth columns of the table. (The measured frequency bands are discussed later in this section.) The upper frequency of each lowpass band (e.g., 450 MHz for Band 1) is chosen to be less than twice the lowest f_0 value so that no harmonics of f_0 are passed to the Tx antenna. The lower frequency of each highpass band (e.g., 900 MHz for Band 2) is chosen to be less than half the lowest $2f_0$ value so that minimal f_0 is passed to the Rx detector.

Table 1 Five sub-bands chosen to realize f_0 = 300 MHz to 2 GHz: the second and fourth columns list the desired (ideal) frequency bands; the third and fifth columns list the measured (actual) frequency bands implemented with back-to-back diplexers.

Band	f_0 Desired	f_0 Measured	$2f_0$ Desired	$2f_0$ Measured
1	300 to 450 MHz	DC to 455 MHz	600 to 900 MHz	536 to 1956 MHz
2	450 to 700 MHz	DC to 695 MHz	900 to 1400 MHz	885 to 2792 MHz
3	700 to 1000 MHz	DC to 1010 MHz	1400 to 2000 MHz	1280 to 3016 MHz
4	1000 to 1500 MHz	DC to 1545 MHz	2000 to 3000 MHz	1735 to 3600 MHz
5	1500 to 2000 MHz	DC to 2464 MHz	3000 to 4000 MHz	2830 to 3470 MHz

To realize deep stopband attenuation (>50 dB) and steep cutoffs for the low and high passbands, diplexers were implemented.[29] As the diplexers provide "forward" paths for both low- and high-frequency outputs, it is possible to squelch reflections that would otherwise cause $2f_0$ to ring back into and out of the PA and/or cause f_0 to ring back toward the Rx antenna and radiate into the environment;[30] this feature is not available when using (typical, commercial) reflective filters.

A novel arrangement of diplexers, a back-to-back configuration, was designed to protect to an even greater degree the output of the PA from reflected harmonics and be easily swappable between Tx and Rx modes. This configuration is shown in Fig. 4.

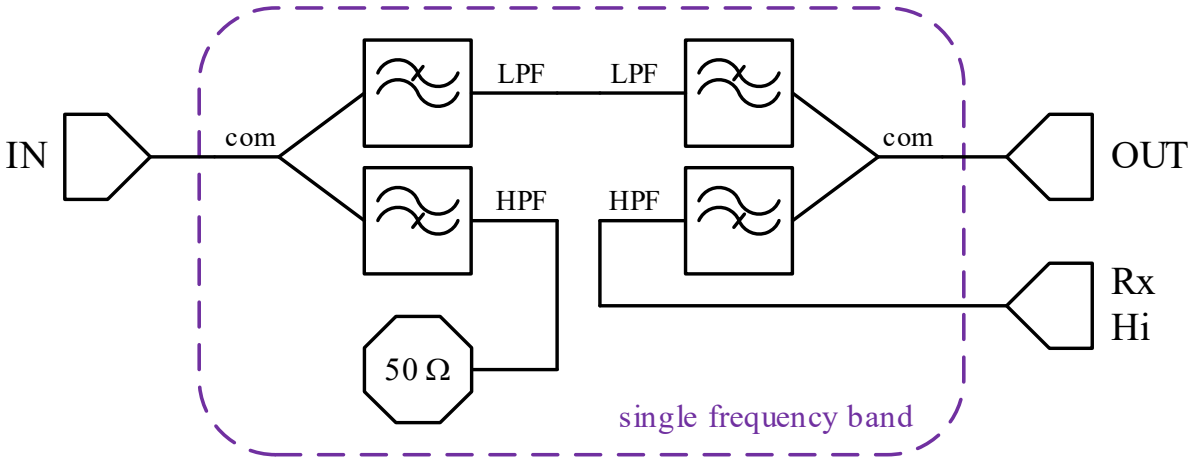

Fig. 4 Flowchart of the back-to-back diplexer configuration for one frequency band (e.g., Band 3)

For a traditional diplexer, the common ("com") port is the input while the LPF and HPF ports are the low- and high-frequency outputs. The present configuration is referred to as "back-to-back" because the low-frequency outputs of two diplexers are tied together; the common port of the first diplexer is the overall input and the common port of the second diplexer is the overall output.

A picture of this configuration, for Band 4, is given in Fig. 5. In the lower portion of the picture is the common port of the first diplexer, which acts as the overall input, labeled "IN". The highpass output of the first diplexer is terminated in a matched load (50 Ω). The lowpass port of the first diplexer is connected directly to the lowpass port of the second diplexer. In the upper portion of the picture is the common port of the second diplexer, which acts as the overall output, labeled "OUT". The highpass port of the second diplexer is available as a secondary output, labeled "Rx Hi". Any back-to-back diplexer pair may be configured for Tx at f_0 or Rx at $2f_0$.

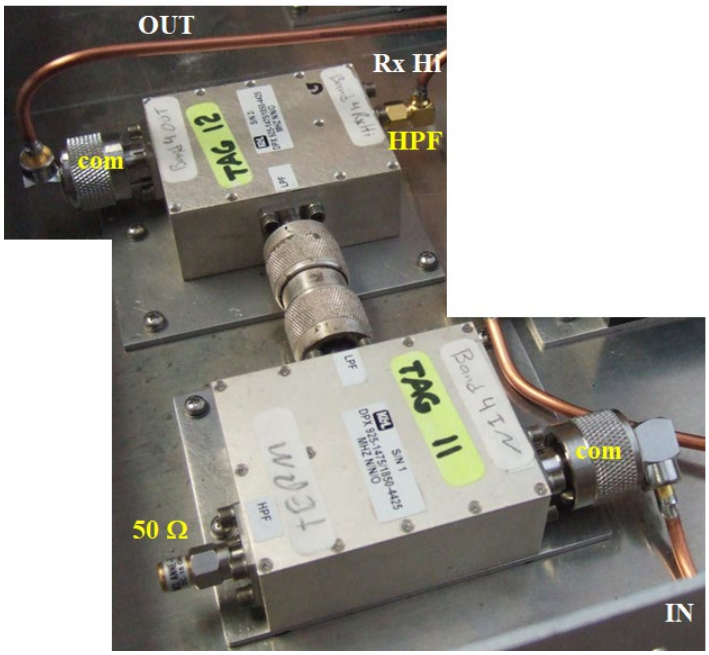

Fig. 5 Picture of the back-to-back diplexer configuration for Band 4

In Tx mode, the diplexer pair is arranged as shown in Fig. 6. An RF signal is generated, amplified, and routed to the "IN" port. The heavily filtered ("linearized") transmit probe leaves the "OUT" port and is sent to the Tx antenna. The "Rx Hi" port is terminated in a matched load. In this manner, any undesired harmonic produced by the PA is sent to the matched load attached to the first diplexer. Also, any harmonic reflected by the target that illuminates the Tx antenna is sent to the matched load attached to the second diplexer (at "Rx Hi").

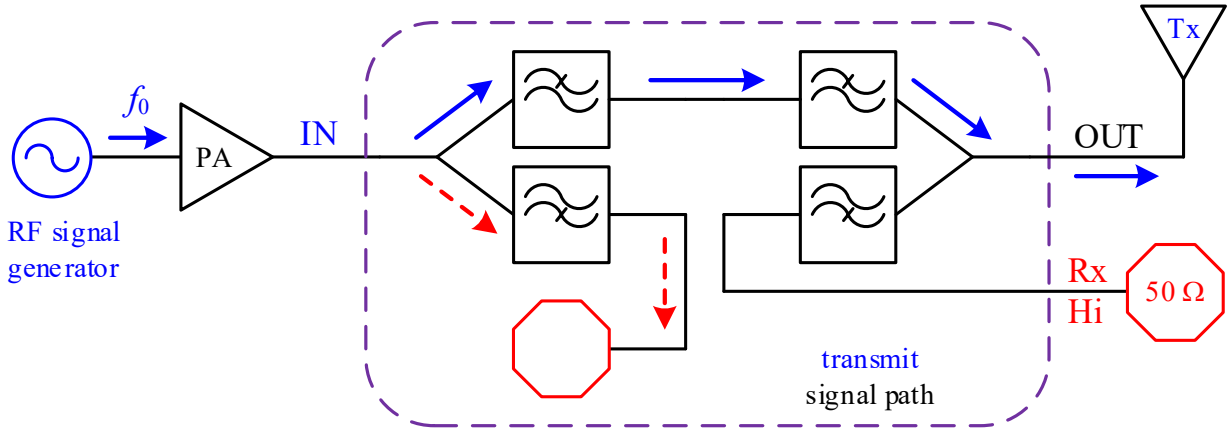

Fig. 6 Back-to-back diplexers configured for high-power transmission (Tx)

In Rx mode, the diplexer pair is arranged as shown in Fig. 7. The target response received by the Rx antenna enters the "OUT" port and is routed to the "Rx Hi" port by the second diplexer. The "IN" port is terminated in a matched load. Any RF at f_0 that has coupled directly from the transmitter into the receiver (via the antennas) is sent to that matched load.

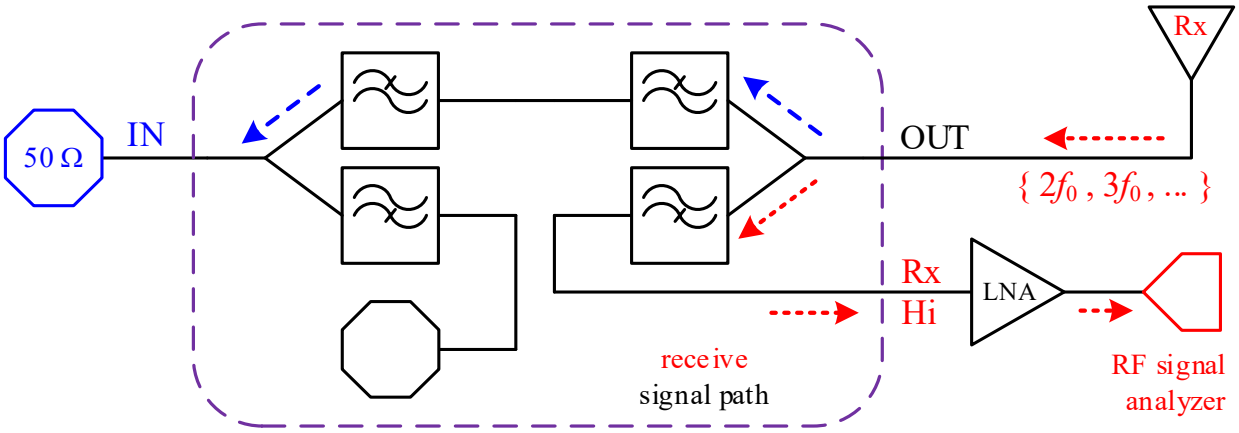

Fig. 7 Back-to-back diplexers configured for low-power reception (Rx)

Diplexer pairs for the bands listed in Table 1 were assembled inside of a large metallic rack-mount project enclosure: 4-U size (19 × 7 × 22 inches). Two boxes were fabricated, to enable simultaneous Tx and Rx using the same (f_0:$2f_0$) frequency band. A picture of the upper tier of one of the boxes is shown in Fig. 8. These diplexer pairs are the higher-frequency bands. The diplexers associated with Band 4 (from Fig. 5) appear in the lower-right-hand corner of this picture. The inputs and outputs for each diplexer pair are routed to the front panel of the box (in the background of this picture) using semi-rigid coaxial cables.

The front connection panel for this box is shown in Fig. 9. This picture is a 180° rotated view of the box in Fig. 8. In Fig. 9, for each frequency band, there are ports labeled "IN" and "OUT", and "Rx Hi", as labeled in Fig. 4.

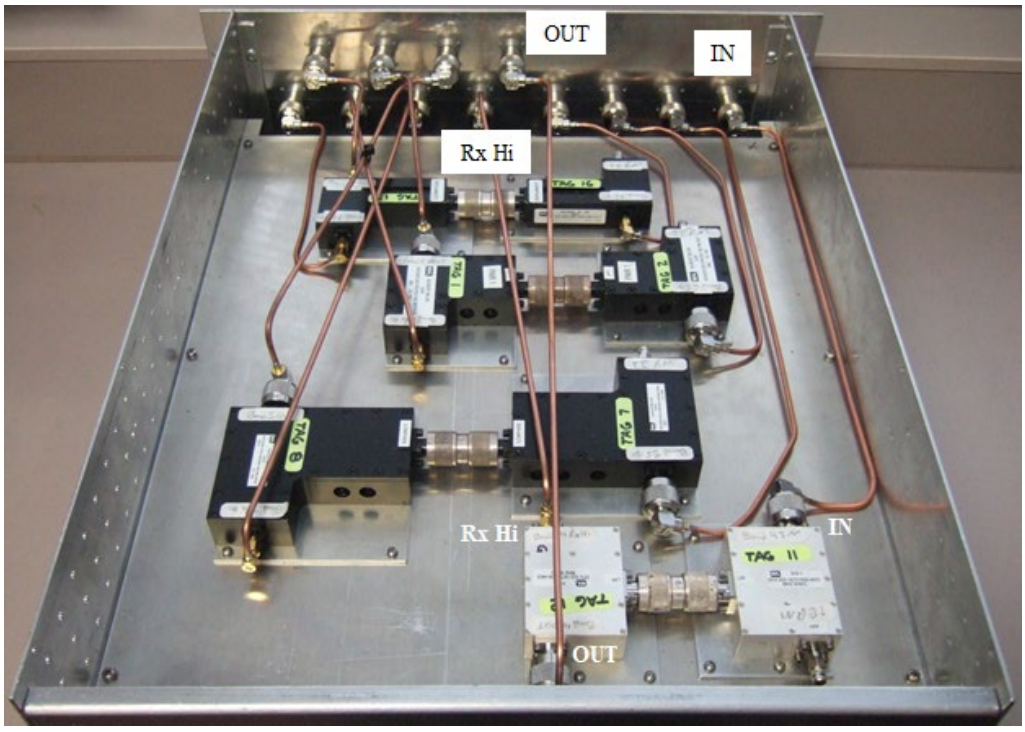

Fig. 8 Picture of the upper tier (higher-frequency) diplexers for the frequencies listed in Table 1

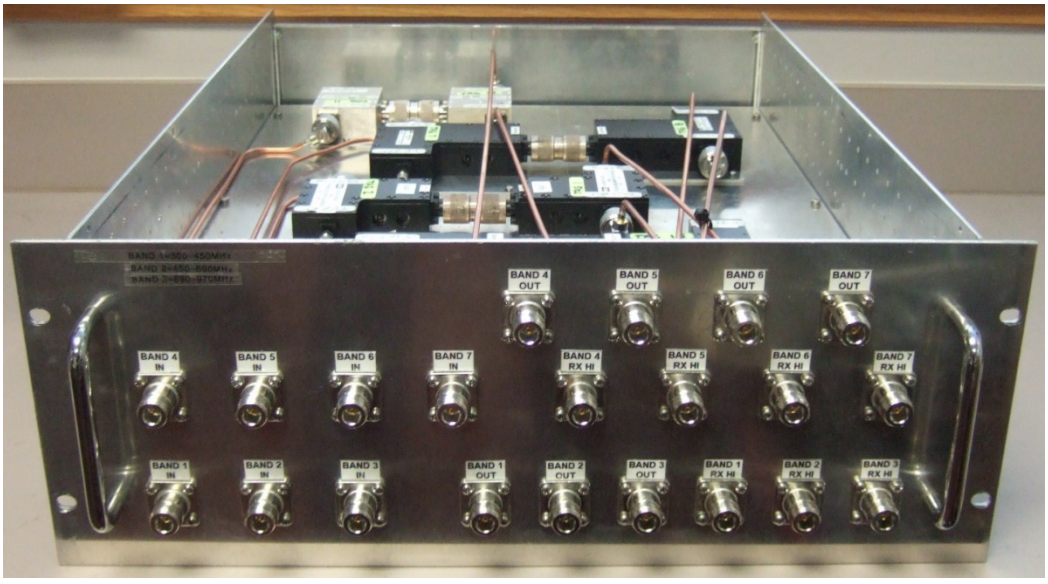

Fig. 9 Front panel for the rack-mount box seen in Fig. 8. Each band has three ports: "IN", "OUT", and "Rx-Hi". For Tx mode, the ports are connected externally as in Fig. 6. For Rx mode, the ports are connected externally as in Fig. 7.

4. S-parameter Measurements for Five Harmonic Frequency Bands

Scattering (*S*) parameter measurements for the bands listed in Table 1, with ports as shown in Fig. 9, were recorded. Two-port transmission parameters (S_{21}) were captured using a SignalHound BB60C analyzer (with a SignalHound TG-44A tracking generator signal source). One-port reflection parameters (S_{11}) were captured using a Keysight N9914A network analyzer. Raw decibel-amplitude *S*-parameter data are provided for Bands 1 through 5 in Figs. 10 through 14, respectively.

The *S*-parameters have been distilled into the "Measured" (third and fifth) columns in Table 1. The passbands (for both f_0 and $2f_0$) are the frequencies for which S_{21} is equal to or greater than –3 dB, while S_{11} is equal to or less than –10 dB (simultaneously). This means that, for all frequencies said to be within the passband for f_0 (in Tx mode), the Tx probe is sent from "IN" to "OUT" with less than 50% power loss, while at least 90% of the harmonic (at $2f_0$) is absorbed internal to the diplexer pair or at the "Rx Hi" matched load. Also, for all frequencies within the passband for $2f_0$ (in Rx mode), the received signal (target response) is sent from "OUT" to "Rx Hi" with less than 50% loss while at least 90% of the residual Tx probe (at f_0) is absorbed at the matched load attached to "IN".

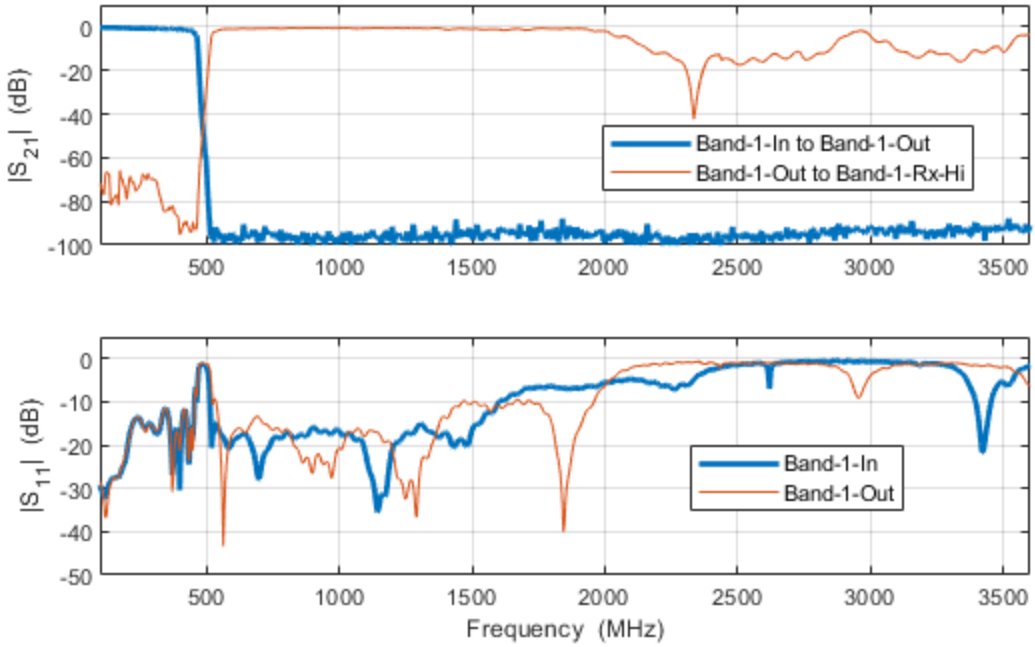

Fig. 10 Transmission and reflection parameters: Band 1

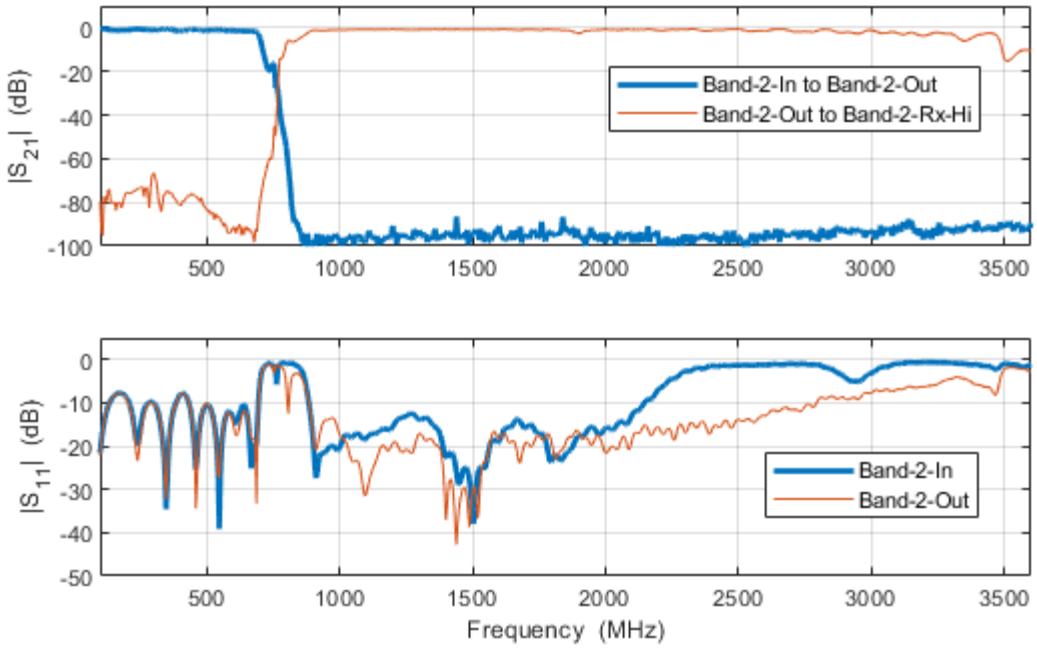

Fig. 11 Transmission and reflection parameters: Band 2

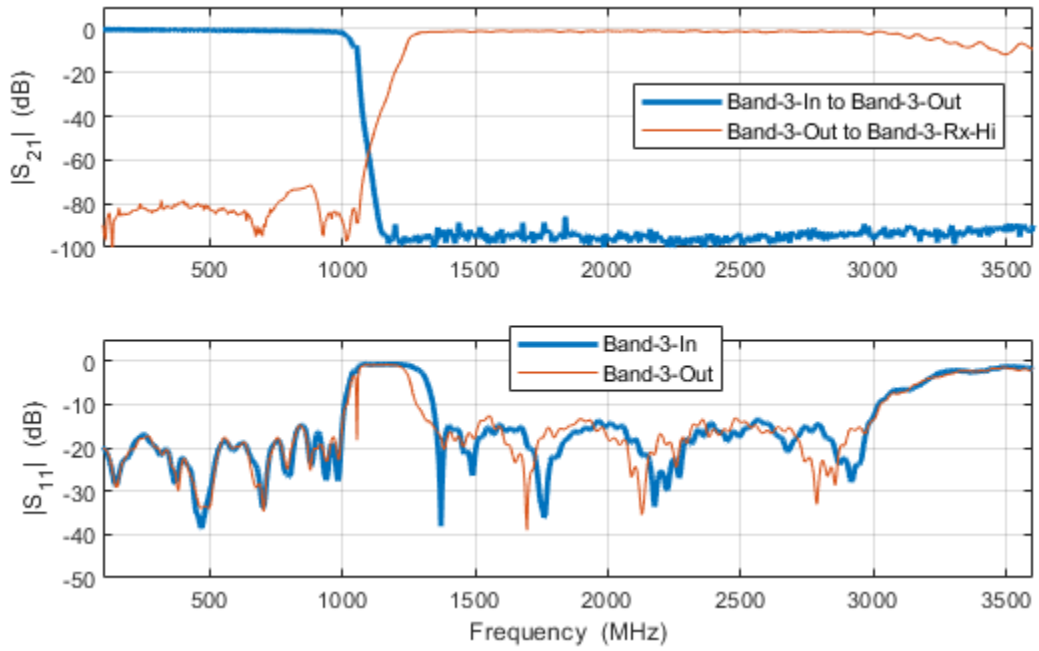

Fig. 12 Transmission and reflection parameters: Band 3

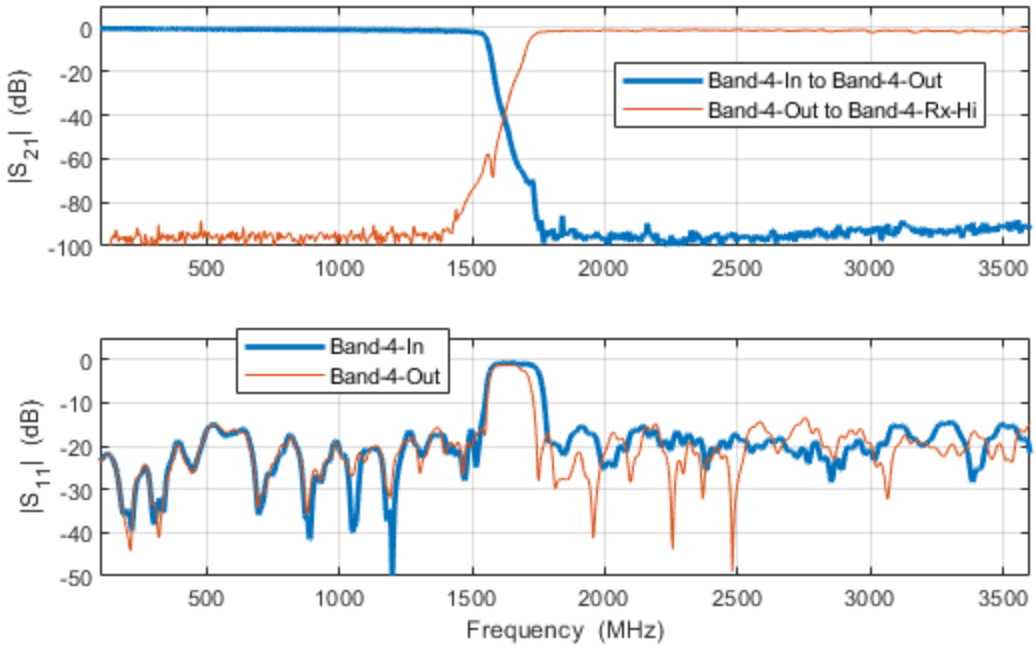

Fig. 13 Transmission and reflection parameters: Band 4

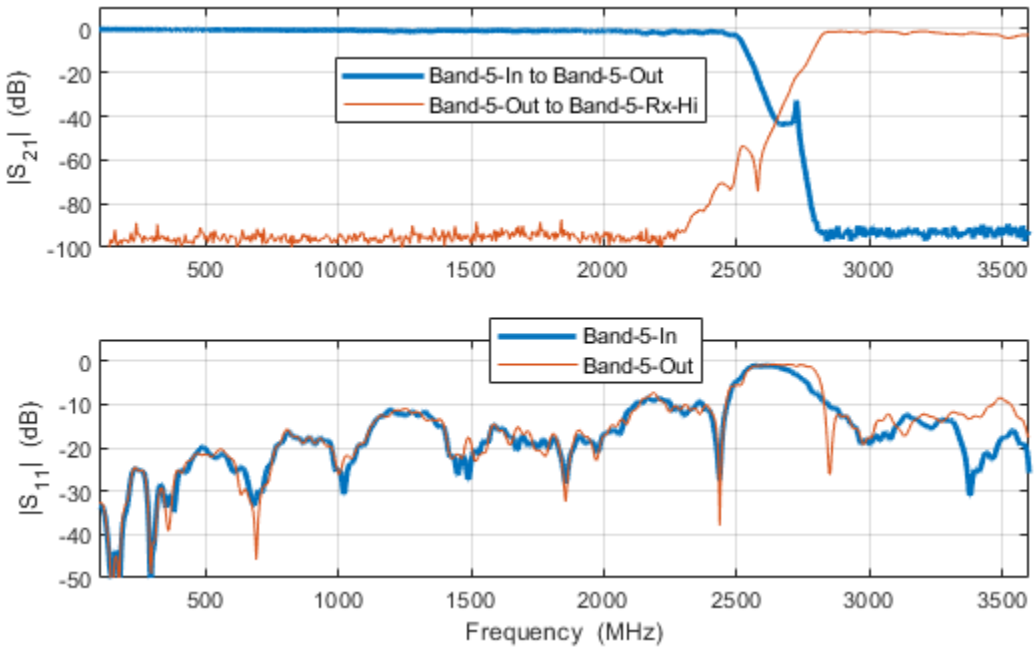

Fig. 14 Transmission and reflection parameters: Band 5

5. Conclusions

A novel arrangement for diplexers, harmonically related and oriented back-to-back, has been implemented to perform NLJD (or "harmonic radar"). To achieve high-power transmission with minimal distortion, the low-frequency probe passes through the lowpass port of two diplexers, while the highpass ports route system-generated harmonics to matched loads. To achieve high sensitivity (low-power reception), the high-frequency target response passes through the highpass port of the second diplexer, while the lowpass ports of both diplexers route the residual low-frequency probe to a matched load.

Figures within this report demonstrate how each diplexer pair may be configured for transmission or reception. Two sets of diplexer pairs have been assembled (i.e., into two 4U rack-mount enclosures) to accomplish simultaneous transmission and reception. These boxes, connected to laboratory instruments and antennas, may be used to probe nonlinear targets of interest for harmonic responses across the ultra-high frequency and long-wave (L) bands.

6. References

1. Aniktar H, Baran D, Karav E, Akkaya E, Birecik YS, Sezgin M. Getting the bugs out. IEEE Microw Mag. 2015 Nov;16(10):40–52.

2. Min KS, Kim JW. Circularly polarized triple band patch antenna for non-linear junction detector. In: Proceedings of the IEEE International Symposium on Antenna Propagation; 2012 July:1–2.

3. Peng Z, Li C. Intermodulation FMCW (IM-FMCW) radar for non-linear wearable targets detection. In: Proceedings of the US National Committee of URSI National Radar Science Meeting; 2018 Jan; Boulder, CO.

4. Raoult J, Martorell A, Chusseau L, Carel C. Intermodulation radar for RF receiver detections. In: Proceedings of the 15th European Radar Conference; 2018 Sep. pp. 273–276.

5. Ivanou M, Chertkov V. Nonlinear junction locator with the possibility of identifying nonlinear objects. In: Proceedings of Materials of VI Junior Research. Conf.; 2014 Apr. pp. 134–137.

6. Pavlik R, Hrubos Z. Cyclostationary and correlation based signal detection for harmonic radar systems. In: IEEE International Symposium Fundamentals Electrical Engineering; 2016 July.

7. Lavrenko A, Cavers J. Two-region model for harmonic radar transponders. Electron Lett. 2020 Aug;56(16):835–838.

8. Rasilainen K, Ilvonen J, A., Hannula JM, Viikari V. Harmonic transponders: Performance and challenges. Progress Electromagn Research M. 2015;41:139–147.

9. Vera GA, Duroc Y, Tedjini S. Third harmonic exploitation in passive UHF RFID. IEEE Trans. Microw Theory Tech. 2015 Sep;63(9):2991–3004.

10. Gruszczynski S, Wincza K. Analog coherent detection in application to high-sensitivity nonlinear junction detectors. In: Proceedings of AFRICON; 2011 Sep. pp. 1–5.

11. Alimenti F, Roselli L. Theory of zero-power RFID sensors based on harmonic generation and orthogonally polarized antennas. Progress in Electromagn. Research. 2013;134:337–357.

12. Kim JW, Min KS, Kim IH, Park CJ. Triple band spiral antenna for non-linear junction detector. In: Proceedings of the International Symposium on Antenna Propagation; 2012. pp. 802–805.

13. Ilbegi H, Hayvaci HT, Yetik IS, Yilmaz AE. Distinguishing electronic devices using harmonic radar. In: IEEE Radar Conference; 2017 May. p. 1502–1505.

14. Kosinski JA, Palmer WD, Steer MB. Unified understanding of RF remote probing. IEEE Sensors. 2011 Dec;11(12):3055–3063.

15. Gallagher KA, Mazzaro GJ, Martone AF, Sherbondy KD Narayanan RM. Derivation and validation of the nonlinear radar range equation. Proc SPIE. 2016 Apr;9829:98290P(1–13).

16. Mazzaro GJ, Martone AF, McNamara DM. Detection of RF electronics by multitone harmonic radar. IEEE Trans Aerosp Electron. Sys. 2014 Jan;50(1)4.

17. Dardari D. Detection and accurate localization of harmonic chipless tags. EURASIP J Adv Signal Process. 2015 Aug;77:1–13.

18. Mazzaro GJ, Martone AF, Gallagher KA, Narayayan RM, Sherbondy KD. Maximizing harmonic-radar target response: Duty cycle vs. peak power. In: Proceedings of the IEEE SoutheastCon; 2016 Apr.

19. Gallagher KA, Mazzaro GJ, Sherbondy KD, Narayanan RM, Martone AF. Automated cancellation of harmonics using feed-forward filter reflection for radar transmitter linearization. Proc SPIE. 2014 May;9077:907703(1–10).

20. Gallagher KA, Narayanan RM, Mazzaro GJ, Sherbondy KD. Linearization of a harmonic radar transmitter by feed-forward filter reflection. Proc IEEE Radar Conf. 2014 May:1363–1368.

21. Jau PH, Tsai ZM, Kuo NC, Kao JC, Lin KY, Chang FR, Yang EC, Wang H. Signal processing for harmonic pulse radar based on spread spectrum technology. IET Radar Sonar Navig. 2014 Mar;8(3):242–250.

22. Tsai ZM, Jau PH, Kuo NC, Kao JC, Lin KY, Chang FR, Yang EC, Wang H. A high-range-accuracy and high-sensitivity harmonic radar using pulse pseudorandom code for bee searching. IEEE Trans. Microw Theory Techn. 2013 Jan;61(1):666–675.

23. Aumann H, Kus E, Cline B, Emanetoglu NW. A low-cost harmonic radar for tracking very small tagged amphibians. In: Proceedings of the IEEE International Instrumentation Measurement Technology Conference; 2013 May. p. 234–237.

24. Hsu ML, Liu TH, Yang TC, Jhan HC, Wang H, Chang FR, Lin KY, Yang EC, Tsai ZM. Bee searching radar with high transmit–receive isolation using pulse pseudorandom code. IEEE Trans Microw Theory Tech. 2016 Dec;64(12):4324–4335.

25. Singh A, Lubecke V. Respiratory monitoring and clutter rejection using a CW Doppler radar with passive RF tags. IEEE Sensors. 2012 Mar;12(3):558–565.

26. Aumann HM, Emanetoglu NW. A wideband harmonic radar for tracking small wood frogs. In: IEEE Radar Conference; 2014 May. pp. 108–111.

27. Gallagher KA, Mazzaro GJ, Martone AF, Sherbondy KD, Narayanan RM. Filter selection for a harmonic radar. Proc SPIE, 2015 Apr;9461:94610A(1–11).

28. Mazzaro GJ, Sherbondy K. Filter selection for a wideband harmonic radar. In: Proceedings of the IEEE SoutheastCon; 2019 Apr.

29. Gallagher KA. Harmonic radar: Theory and applications to nonlinear target detection, tracking, imaging and classification [doctoral dissertation]. [State College (PA)]: The Pennsylvania State University; 2015 Dec.

30. Mazzaro GJ. Nonlinear junction detection vs. electronics: System design and improved linearity. In: Proceedings of the IEEE International Radar Conference; 2020 Apr; Washington, DC.

List of Symbols, Abbreviations, and Acronyms

CW	continuous-wave
EM	electromagnetic
HPF	highpass filter
L	long-wave
LNAs	low-noise amplifiers
LPF	lowpass filter
NLJD	nonlinear junction detection
PA	power amplifier
RF	radio-frequency
Rx	receive
SNR	signal-to-noise ratio
Tx	transmit

1 (PDF)	DEFENSE TECHNICAL INFORMATION CTR DTIC OCA
1 (PDF)	CCDC ARL FCDD RLD DCI TECH LIB
8 (PDF)	CCDC ARL FCDD RLS RM K GALLAGHER D HARVEY G KIROSE G MAZZARO K SALIK K SHERBONDY A SULLIVAN FCDD RLS G A HARRISON